Fig. 1. Syngenetic pyrogenic tree mould cave in the lava flow – the lower part of Funatsu Tainai Cave, Mt. Fuji, Japan. Photo P. Bella (p. 8).

Fig. 2. Epigenetic tree mould cave in volcaniclastic rocks – Dwarf´s Cave, Krupina Plateau, Slovakia. Photo P. Bella (p. 8).

Fig. 3. Epigenetic tree mould cave in lahar deposits – Skalky skřítků Cave, Doupov Hills, Czech Republic. Photo P. Bella (p. 9).

Fig. 5. Lava wall ribbed surface of syngenetic pyrogenic tree mould cave – the upper part of Funatsu Tainai Cave, Mt. Fuji, Japan. Photo P. Bella (p. 9).

Fig. 4. Epigenetic tree mould cavity in the travertine mound – Jazierce, the eastern foot of Great Fatra Mts., Slovakia. Photo P. Bella (p. 9).

Fig. 4. Ferenc (Francis) Cave near Sopron. Photo I. Eszterhás (p. 15).

Fig. 6. Kő Hole (Rockhole) near the Kishartyán village. Photo I. Eszterhás (p. 17).

Fig. 7. The Főág (Head Passage) of the Betyár (Outlaw) Cave in Szentkút. Photo I. Eszterhás (p. 17).

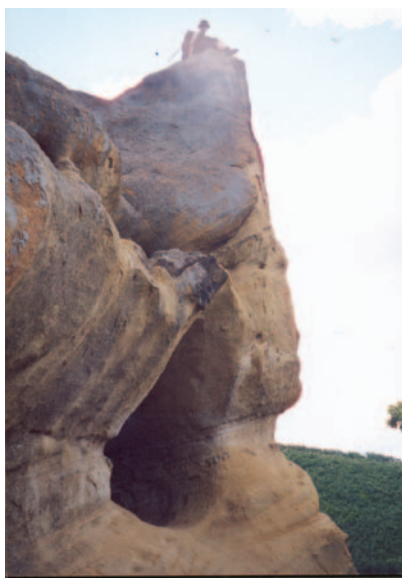

Fig. 9. The Nagy-Lyukas-kő Cave (Big Holed Rock) near Ivád. Photo I. Eszterhás (p. 18).

Fig. 11. The Mókus Bácsi Cave (Uncle Squirrels Cave) in the Mátra Mountains. Photo I. Gönczöl (p. 19).

Fig. 2. Kattarellikivi (Chantarelle rock) at Liljendal. Mushroom like marine shore stack. Photo S. Kielosto (p. 32).

Fig. 3. Jättehandtaget (Giant's handle) at Saltvik. Rock arch-like marine shore stack. Photo R. Lounema (p. 33).

Fig. 4. Raised beaches on the marine boulder field at Vammavaara, Tervola. Photo was taken on the top of the low shore stack-tor. Photo P. Johansson (p. 34).

Fig. 5. Maljakivet (Rock Bowls) at Joutsa. Four lake shore stacks and the marine cave between them. Photo T. Herttua (p. 35).

Fig. 6. Rock nubbins similar to lake shore stacks at Ruskeapää, Nokia. Photo A. Kejonen (p. 36).

Fig. 7. Pirunportti (Devils Gate) at Putelo, Rantasalmi. Boulder arch-like lake shore stack on the ancient beach of the Suursaimaa (Great Saimaa). Photo A. Kejonen (p. 36).

Fig. 8. One of the lake shore stacks of the Lake Inari, Finnish Lapland. Photo O. Sälevä (p. 36).

Fig. 10. Weathering pits at Pihtipudas. Photo A. Tiainen (p. 38).

Fig. 1. Cave type 1 developed along a major fracture plane, (Serra de Galiñeiro, Pontevedra, Spain). Photo J.R. Vidal Romani, M. Vaqueiro (p. 42).

Fig. 9. Rupakivi at Salla. The best known river shore stack in Finland. Photo P. Johansson (p. 37).

Fig. 2. Cave type 2 associated with a residual blockfield (Serra de Galiñeiro, Pontevedra, Spain). Photo J.R. Vidal Romani, M. Vaqueiro (p. 42).

Fig. 3. Cave type 3. Boulder tafone. (Monte Louro, Coruña, Spain). Photo J.R. Vidal Romani, M. Vaqueiro (p. 43).

Fig. 6. Flowstone of opal-A (pigotatite) from O Folón Cave (Pontevedra, Spain). Photo J.R. Vidal Romani, M. Vaqueiro (p. 44).

Fig. 4**.** The hole after an eroded intraclast in the sandstone bed (Mamčina galéria - Mummy´s Gallery, Spišská branch of the Jaskyňa pod Spišskou cave). Photo M. Kováčik, J. Bóna (p. 50).

Fig. 4. Opal-A stalactite (Castelo da Furna, Boivão, Portugal). Photo J.R. Vidal Romani, M. Vaqueiro (p. 43).

Fig. 7a. Macro gour or drip pool of opal-A (pigotite) from O Folón Cave (Pontevedra, Spain). Photo J.R. Vidal Romani, M. Vaqueiro (p. 44).

Fig. 5. Groove casts and 4 cm long straw stalactite at the bottom bedding plane of the sandstone (Spišská branch of the Jaskyňa pod Spišskou cave). Photo M. Kováčik, J. Bóna (p. 50).

Fig. 8. Jaskyňa pod Spišskou – the entrance shaft. Photo M. Hajduk (Speleoclub Šariš) (p. 53).

Fig. 9. The entrance of cave No. 6, The Big Cave or Te Ana Ru. In the foreground the intruding dune sand. Photo G. Szentes (p. 74).

Fig. 5. The entrance of cave No. 2. Photo G. Szentes (p. 72).

Fig. 7. The passage in cave No. 5 follows a NE-SW trending fault. Photo G. Szentes (p. 73).

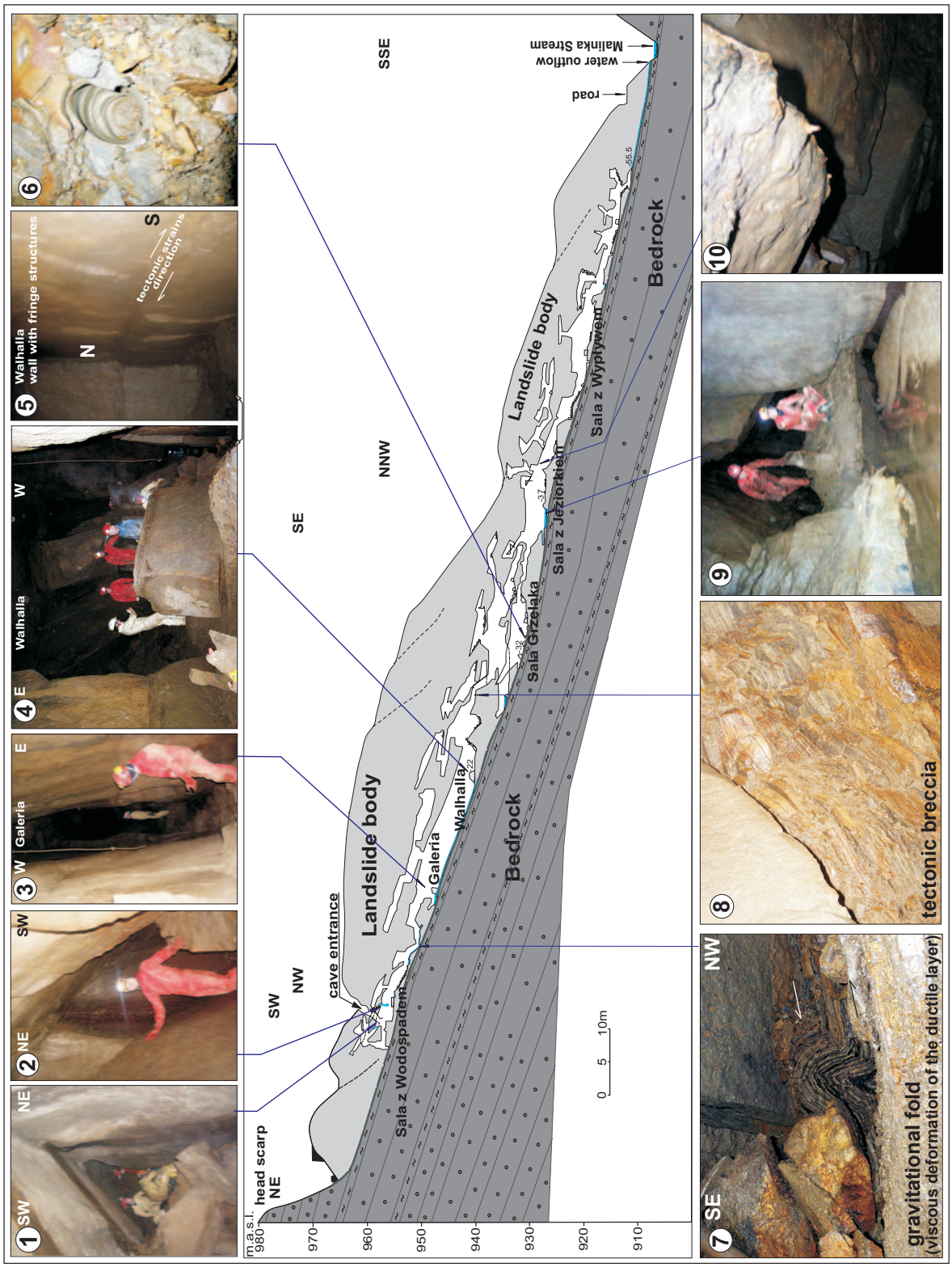

Fig. 3. Longitudinal cross section of the Jaskinia Miecharska cave and landslide, with photos of typical passages, as well as unique forms and phenomena in the cave. Explanation of symbols - see Fig. 1. Description of photos in the text. Photos W. Margielewski, J. Urban (p. 62).

Fig. 10. The large abrasion chamber in cave No. 6. Photo G. Szentes (p. 74).

Fig. 12. The gradually narrowing passage in cave No. 8. Photo G. Szentes (p. 75).

Fig. 14. The contrast between the landscape 95 years ago and today (edited by G. Szentes). A. In the 1910 the sea broke against the cliffs just north of the Whatipu and the Piha Tramway was built on trestles across the mouths of the caves (after Cameron et al. 1997). B. and C. Since than (today) a 1 km wide sand flat has grown out in front of the cliffs. Photo G. Szentes (p. 76).

Fig. 13. The abrasion chamber in cave No. 9. Photo G. Szentes (p. 75).

Fig. 3. The sandstone in the face of the abandoned pit in Grudziądz bears numerous lenses of loose sand. The largest lens at the bottom of the pit face is the entrance and upper passage of the Jaskinia pod Wierzbą cave. Photo J. Urban (p. 88).

Fig. 2. Cavities of the Jaskinia w Połchowie cave formed due to gravitational removal of loose sand from the sandstone body situated on a steep slope of the valley. Photo J. Urban (p. 87).

Fig. 7. The calcite flowstone in the Bajka II cave sampled for the U/Th analysis (sample BA-3). Photo J. Urban (p. 90).

Fig. 6. Characteristic elements of the gully and caves Bajka I and II: A – natural sandstone face on the gully slope with the caves' entrances; B – the interior of Bajka I cave, C – spring (water outflow) in the lower part of the gully. Photo J. Urban (p. 89).

Fig. 9. The colonnade of the sandstone pillars in the entrance of the Jaskinia w Mechowie cave; the artificial (concrete) pillar underpinning the ceiling is situated just behind the lady. Photo J. Urban (p. 91).

Fig. 10. The gallery of the Jaskinia w Mechowie cave, near the dome-like structure; the walls are covered with the calcite flowstones. Photo J. Urban (p. 91).

Fig. 12. The chamber in the Jaskinia Śpiącego Szweda cave, formed within the boulder clay; rock clasts covered with thin white calcite crusts are visible in the clay. Photo J. Urban (p. 92).

Fig. 11. The entrance to the Schron w Cyplu cavity, formed in the boulder clay on the level of the beach, due to storm wave activity. Photo J. Urban (p. 92).

Fig. 14. The entrance to the small chamber in the Jaskinia Goryla cave. Photo J. Urban (p. 93).

Fig. 1 NNR Adršpašsko-teplické skály – the largest and the best developed rock city in the Czech Republic. Photo O. Jenka (p. 96).

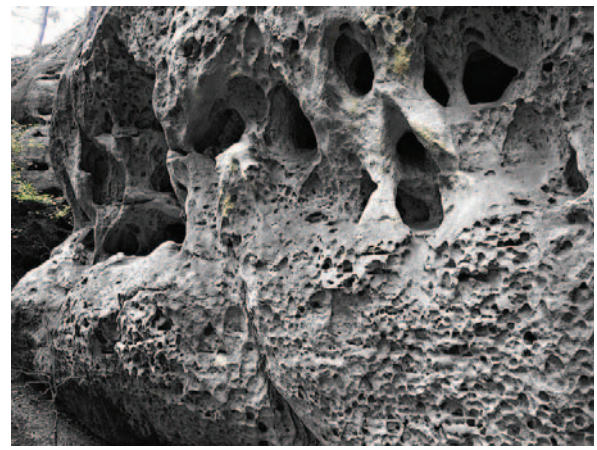

Fig. 4. Honeycombs and cavernous weathering in the Upper Cretaceous sandstones in NM Husa. Photo O. Jenka (p. 97).

Fig. 3. Rock walls of the Labe R. canyon in PLA Labské pískovce dissected by gorges. Photo O. Jenka (p. 97).

Fig. 6. A weathering pit in the Upper Cretaceous sandstones in NNR Broumovské stěny in PLA Broumovsko. Photo O. Jenka (p. 98).

Fig. 7. A rock window in the Upper Cretaceous sandstones – the locality of Svídnická věž in the PLA Broumovsko. Photo O. Jenka (p. 98).

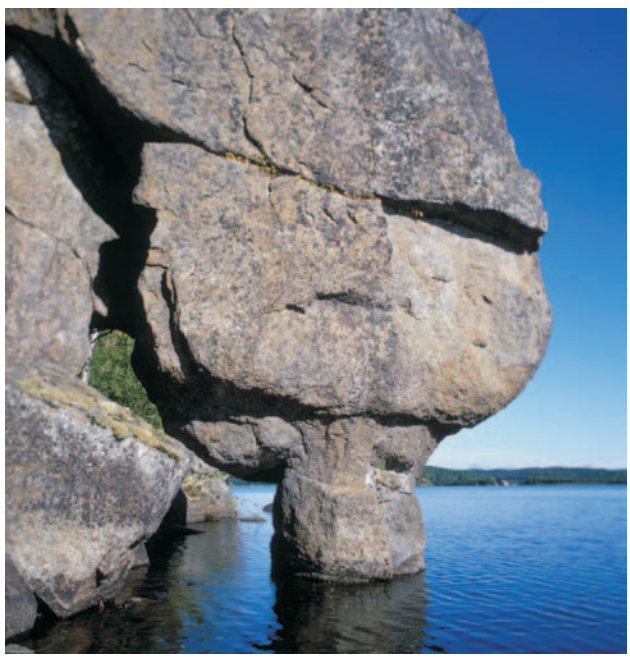

Fig. 1. *Saarnastuoli* (Vicar's pulpit). Famous lake shore stack at cape Kynsikaivonniemi, Lake Puulavesi. Photo J. Väätäinen (p. 104).

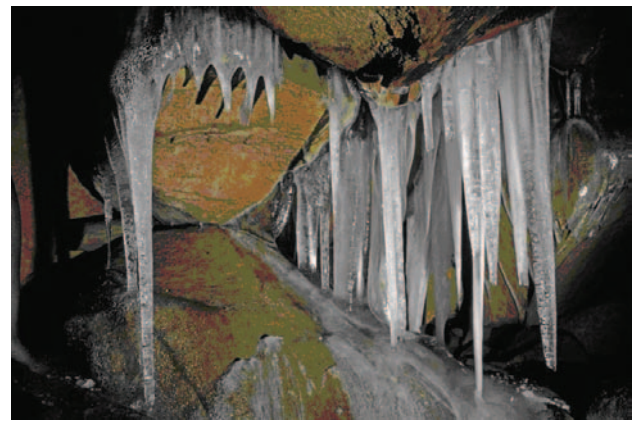

Fig. 9. The largest and longest boulder cave in Czechia – the protected Teplická jeskyně Cave in the PLA Broumovsko. Photo O. Jenka (p. 99).

Fig. 3. *Alttarikallio* Altar rock). Shore stacks and beach caves at cape Kynsikaivonniemi, Lake Puulavesi. Beach caves have formed between the shore stacks. Photo J. Väätäinen (p. 104).

Fig. 2. Extraordinary form - stalactite (?) in the Jaskinia Dująca cave. Photo Cz. Szura (p. 111).

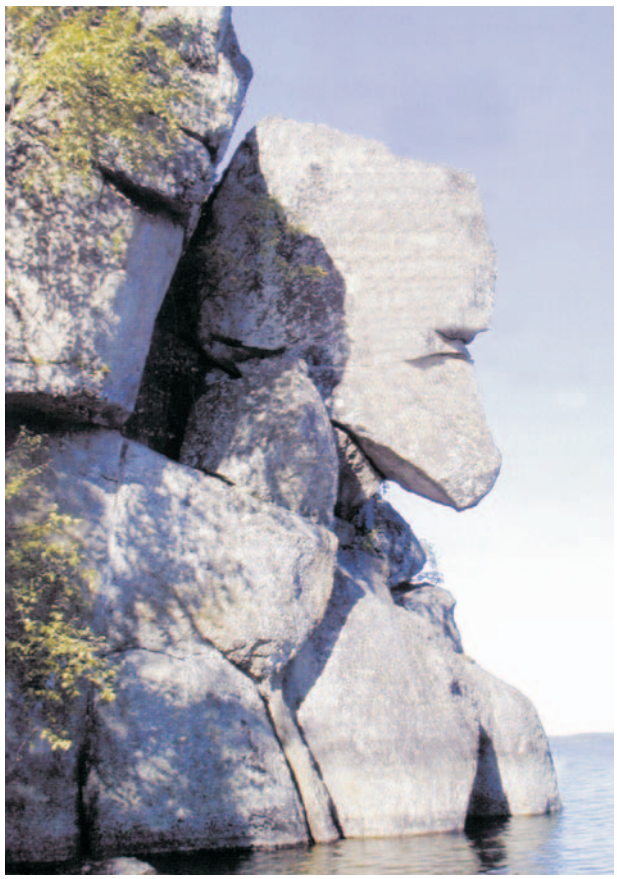

Fig. 2. *Karhu* (Bear). Famous lake shore stack at cape Kynsikaivonniemi, Lake Puulavesi. Karhu is the ancient fishing god used until about 1890-1900 AD. Photo J. Väätäinen (p. 104).

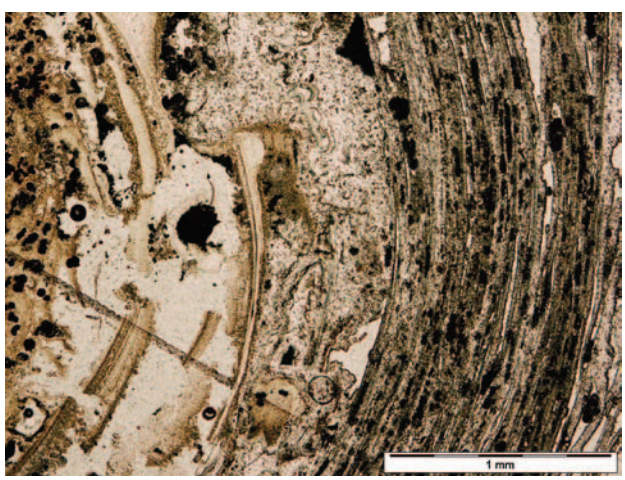

Fig. 5. External and intermediate parts of the stalactite in the Jaskinia Wiślańska cave. The stalactite is composed of light grey silica (amorphous with a small participation of quartz – see fig. 5) and dark brown particles of organic substance. Transmitted light, one polar. Photo M. Schejbal-Chwastek (p. 112).

Fig. 3. Cross-section of the stalactite 2.5 cm long from the Jaskinia Dująca cave. The central part is composed of white, non-compacted material with round aggregates and dark brown organic material, whereas the external envelope is harder and displays lamination. Photo J. Urban (p. 111).

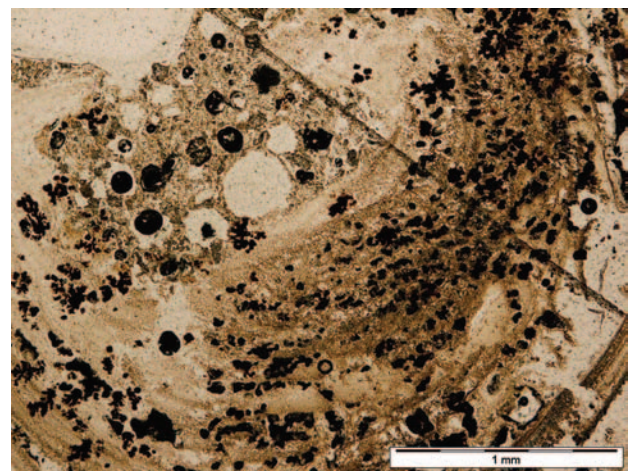

Fig. 6. An internal part of the stalactite in the Jaskinia Wiślańska cave. The stalactite is composed of light grey silica (amorphous with small particles of quartz – see fig. 5) and dark brown particles of organic substance. Transmitted light, one polar. Photo M. Schejbal-Chwastek (p. 112).

Fig. 7. Crenulated flowstone covering the ceiling and grading into range of tooth-like forms on its edge, the Jaskinia Dująca cave. Photo Cz. Szura (p. 113).

Fig. 8. Calcite moonmilk on the ceiling of the gallery of the Jaskinia Dująca cave. Photo Cz. Szura (p. 113).

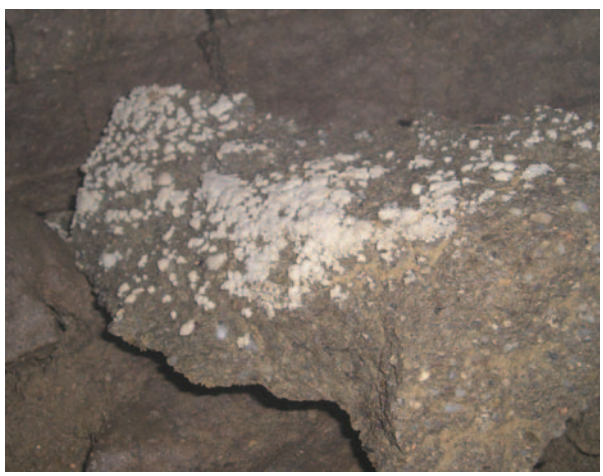

Fig. 10. Crusts of cauliflower-like calcite speleothems on the sandstone block in the Jaskinia Wiślańska cave. Photo Cz. Szura (p. 113).

Fig. 9. Calcite mushrooms (bushes) ca 1 cm high with marked their basement, the Jaskinia Wiślańska cave. Photo J. Urban (p. 113).

Fig. 11. Gypsum-calcite coating on the vertical wall of the Walhalla chamber in the Jaskinia Miecharska cave; the horizontal size of the formation is 2-3 m. Photo J. Urban (p. 114).

Fig. 12. Gypsum crusts (crystal clusters) on the surface of a sandstone block in the Jaskinia Wiślańska cave; the largest crystal is several millimetres long. Photo Cz. Szura (p. 114).

Fig. 13. Calcite helictite 2-3 cm long, on the vertical wall of the Grzelak chamber in the Jaskinia Miecharska cave. Photo J. Urban (p. 114).

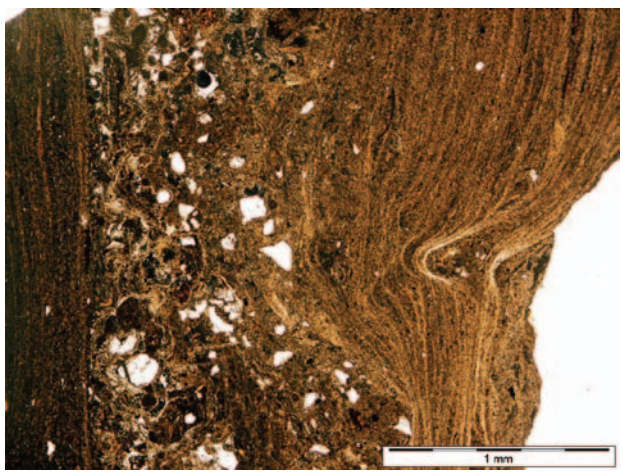

Fig. 15. A transversal cross-section of the mineral crust in the Diabla Dziura cave. The crust is composed mainly of clay minerals and amorphous siliceous material, but in the central part, detrital quartz rains also occur. Transmitted light, one polar. Photo M. Schejbal-Chwastek (p. 115).

Fig. 14. Mineral crust with corraloidal and botryoidal forms on the wall of the Diabla Dziura cave; the forms are less than 1 cm. Photo J. Urban (p. 114).

Fig. 4. Calcite stalactites tilted owing to the gravitational mass movements postdating their formation, Korytarz Naciekowy gallery in Jaskinia Słowiańska-Drwali cave. Photo T. Mleczek (p. 122).

Fig. 5. The calcite draperies ended with a range of soda straw stalactites in the Jaskinia Stalaktytowa cave; also the spider's cocoon of the *Meta* genus is visible. Photo J. Urban (p. 122).

Fig. 7. Speleothems sampled in the Jaskinia Słowiańska-Drwali cave. A – sample 1, B – sample 2. Photo W. Margielewski (p. 123).

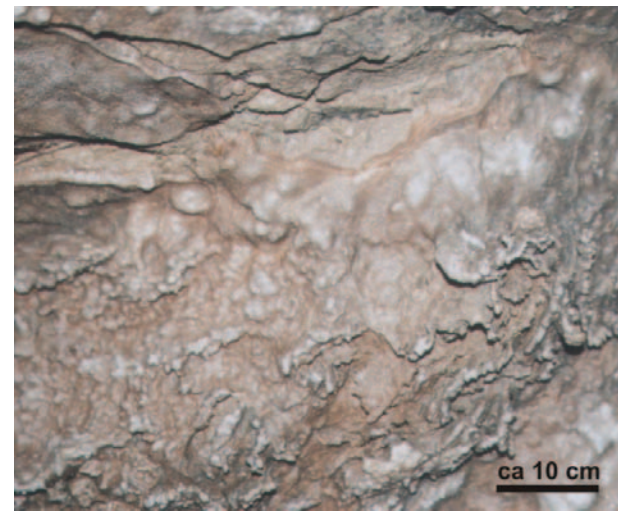

Fig. 6. The calcite flowstone with small corraloid and irregular forms; Sala Błotna chamber of Jaskinia Słowiańska-Drwali cave. Photo W. Margielewski (p. 123).

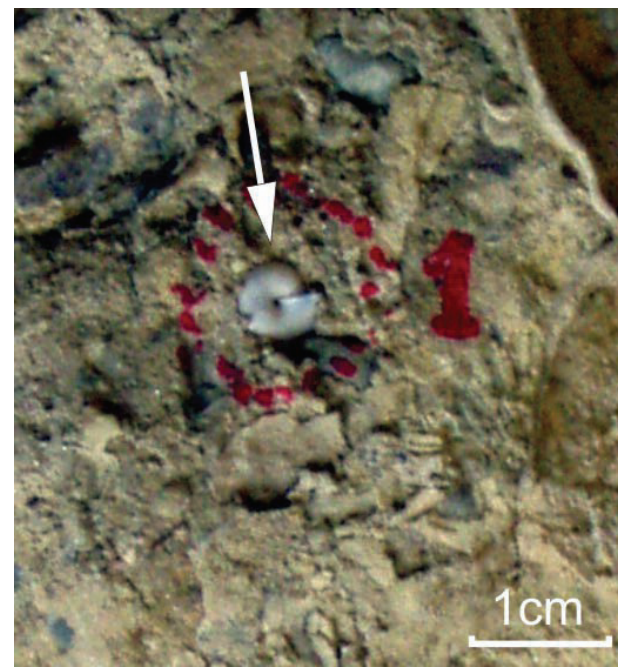

Fig. 10. Snail (pointed by arrow) and other detrital material in the flowstone from Jaskinia Słowiańska-Drwali. Photo W. Margielewski (p. 124).